frontiers | Frontiers in Earth Science

TYPE Original Research
PUBLISHED 28 April 2025
DOI 10.3389/feart.2025.1572136

OPEN ACCESS

EDITED BY
Zhentao Dong,
China University of Petroleum, China

REVIEWED BY
Shansi Tian,
Northeast Petroleum University, China
Min Wang,
China University of Petroleum, China
Taohua He,
Yangtze University, China

*CORRESPONDENCE
Youzhi Wang,
76553188wyz@sina.com

RECEIVED 06 February 2025
ACCEPTED 24 March 2025
PUBLISHED 28 April 2025

CITATION
Wang Y, Wang X, Chen X, Li X, Wu J, Gao X, Peng J, Wang B, Xie Y and Wu H (2025) Classification and origin of pore–throat systems in tight sandstone reservoirs: a case study of the Xujiahe Formation in the Northeastern Sichuan Basin, China. *Front. Earth Sci.* 13:1572136. doi: 10.3389/feart.2025.1572136

Classification and origin of pore–throat systems in tight sandstone reservoirs: a case study of the Xujiahe Formation in the Northeastern Sichuan Basin, China

Youzhi Wang[1,2]*, Xiandong Wang[1,2], Xuqiang Chen[1,2], Xiaohui Li[1,2], Jingfeng Wu[1,2], Xiang Gao[1,2], Jianliang Peng[1,2], Biao Wang[1,2], Yingyi Xie[1,2] and Haiguang Wu[3]

[1]Exploration and Development Research Institute of Daqing Oilfield Company Ltd., Daqing, Heilongjiang, China, [2]National Key Laboratory of Green Exploitation of Continental Shale Oil with MultiResource Collaboration, Daqing, Heilongjiang, China, [3]School of Geosciences, Northeast Petroleum University, Daqing, China

Introduction: The reservoirs of the Xujiahe Formation in the northeastern Sichuan Basin have complex rock components, strong pore–throat inhomogeneity, and large differences in the production capacity between wells, and the mechanism of high-quality pore–throat development must be clarified to support well deployment.

Methods: Taking the tight sandstone reservoirs of the Xu-2 member of the Xujiahe Formation as the research object, this study establishes a pore–throat system classification, reveals the origins of various pore–throat systems, and conducts a microscopic analysis of the pore structure through thin sections, mercury intrusion capillary pressures, and nuclear magnetic resonance studies.

Conclusion: The results show that four main types of reservoir spaces can be found in the cast thin section, namely primary InterP pores, residual InterP pores, dissolution pores, and IntraP pores. By observing the cast thin section, the pore–throat system can be classified into three categories: InterP pore–throat systems, mixed InterP-dissolutional pore–throat systems, and dissolution-IntraP pore–throat systems. The pore–throat systems of the reservoir are controlled by both the sedimentary environment and diagenesis, strong hydrodynamics, high quartz grain contents, low mud and calcareous clast contents, and moderate amounts of volcanic clasts that are favorable for chlorite film formation. A large number of intergranular pores are efficiently maintained, forming an intergranular pore–throat system with the best storage conditions. The research results can guide the study of the formation mechanism of the tight reservoirs in this area and also provide some reference for the evaluation of reservoir consistency.

KEYWORDS

tight sandstone, pore–throat systems, reservoir origin, Xujiahe Formation, Sichuan Basin

1 Introduction

Tight sandstone gas, as an unconventional natural gas resource, has gained the attention of scholars at home and abroad (Garcia-Hidalgo et al., 2007; Li J. et al., 2024; Li P. et al., 2024). More than 70 basins around the world have been found or are presumed to contain tight sandstone gas, mainly in North America, Europe, and Asia (Mount, 1984; He et al., 2023). However, tight sandstone gas reservoirs in China have been discovered mainly in the Sichuan Basin, Ordos Basin, and Junggar Basin. The tight sandstone reservoirs of the Xujiahe Formation in the Sichuan Basin are famous for their strong reservoir inhomogeneity (Deng et al., 2022; Jiang et al., 2023). Scholars have previously conducted numerous studies on lithologic delineation, depositional models, and reservoir classification of tight sandstones (Chen et al., 2024; Guan et al., 2024), but studies on the quantitative identification of pore–throat systems in tight sandstone reservoirs are rare. The tight sandstone of the Xujiahe Formation is composed of feldspar, quartz, and rock fragments, and diagenesis and sedimentary microfacies affect the pore structure (Liu et al., 2020). When these influencing factors are clearly studied, the formation mechanism and sweet-spot control factors of the tight sandstone reservoirs can be effectively revealed mechanistically. However, only the microstructures of several major lithologies in tight sandstones have been characterized and compared, and the influence of diagenesis on the pore–throat systems has not been systematically revealed (Li et al., 2019).

In addition, the pore–throat structure of tight sandstone gas reservoirs is complex, and the superposition of different pore–throat types may correspond to similar characterization parameters (e.g., particle size, pore size, and pore–throat size distribution), which makes it difficult to fully reveal the microstructural differences in tight sandstone (Liu X. et al., 2024; Hu et al., 2024; Hu et al., 2022). Pore–throat systems are network systems that consist of pore spaces in the rock and the throats that communicate with them, with a certain degree of connectivity (Dong et al., 2025; Dong et al., 2024). For tight sandstone reservoirs, the influence of complex diagenesis and deposition leads to the formation of diverse pore–throat systems, and similar pore–throat distributions may correspond to different pore–throat combination relationships (Jiang et al., 2015; Lai et al., 2018a). Therefore, the quantitative identification of pore–throat systems should be a breakthrough point to reveal the differences in the pore–throat structure of tight sandstone reservoirs and clarify the factors controlling the development of high-quality reservoirs (Lai et al., 2018b; Liu et al., 2018). Several techniques and methods have been used in the past to elucidate the pore system of tight sandstones (He et al., 2022; Li et al., 2022; He et al., 2018). The pore types, geometries, and sizes within tight sandstones have been qualitatively analyzed via advanced two/three-dimensional imaging techniques such as field emission scanning electron microscopy (FE-SEM), cast thin sections, and mercury injection capillary pressure (MICP) measurements. Among these techniques, MICP is considered an effective method for characterizing the pore structure as it can theoretically probe pores smaller than 3 nm.

Therefore, this work takes the dense sandstone of the Xujiahe Formation in the northeastern Sichuan Basin as an example; combines thin section, FE-SEM, cathodoluminescence (CL) observations, and MICP data to classify and discriminate the pore–throat systems; summarizes the development characteristics and controlling factors of the pore–throat system of tight sandstone; analyzes the influence of diagenesis on the pore–throat systems; and summarizes the evolution pattern of the pore–throat system. This research can not only guide the study of the formation mechanism of tight reservoirs in the study area but can also provide a reference for the correlation between the classification and genetics of pore–throat systems.

2 Geological setting

The Sichuan Basin is located in South China (Figure 1a) and is a crucial hydrocarbon-bearing foreland basin that can be divided into five first-level tectonic units: a low and steep fold belt in southern Sichuan, a high and steep fold belt in eastern Sichuan, a low and gentle belt in the central Sichuan uplift, a low and steep fold belt in western Sichuan, and the Micangshan Daba front thrust belt (Figure 1b) (Wang et al., 2020; Yang et al., 2021). The Yilong–Pingchang area is located in the northeastern Sichuan Basin, whose tectonic direction is mainly north-west, with extrusive and torsional reverse faults developing and with a structural pattern of "a depression between two uplifts" in the plane (Figure 1c). The Xujiahe Formation in the northeastern Sichuan Basin is dominated by continental sediments, including channel facies, delta plain facies, and delta front facies. According to the lithology, combined log features, and sedimentary cycles, the Xujiahe Formation in the northeastern Sichuan Basin is divided into six members from the top to bottom (Xu-1, Xu-2, Xu-3, Xu-4, Xu-5, and Xu-6), with the Xu-1, Xu-3, and Xu-5 members being hydrocarbon source rocks (Figure 1 (D)) (Zhao et al., 2024; Zhang et al., 2024). Of these, the Xu-1 member is characterized by gray mudstone interbedded with thinner coal; the Xu-3 member is characterized by gray mudstone, coal, and sandstone interbedding; and the Xu-5 member is characterized by gray mudstone and sandstone interbedding. Tight sandstone gas reservoirs have developed in the Xu-2, Xu-4, and Xu-6 members, with lithologies of lithic conglomerate, fine sandstone, and medium sandstone.

3 Samples and methods

3.1 Samples

In this study, a total of 114 tight sandstone reservoir samples from the Xu-2 members were collected from the Y1 well in the northeastern Sichuan Basin, South China (Figure 1). A relatively complete experimental reservoir characterization investigation was conducted, including porosity and permeability measurements, thin section casting, scanning electron microscopy (SEM), and MICP. Moreover, the mineral types and diagenesis characteristics are effectively revealed by CL observations.

3.2 Experiments and methods

3.2.1 Porosity and permeability measurements

Two parameters, porosity and permeability, can directly reflect the reservoir storage performance, and they are critical in reservoir

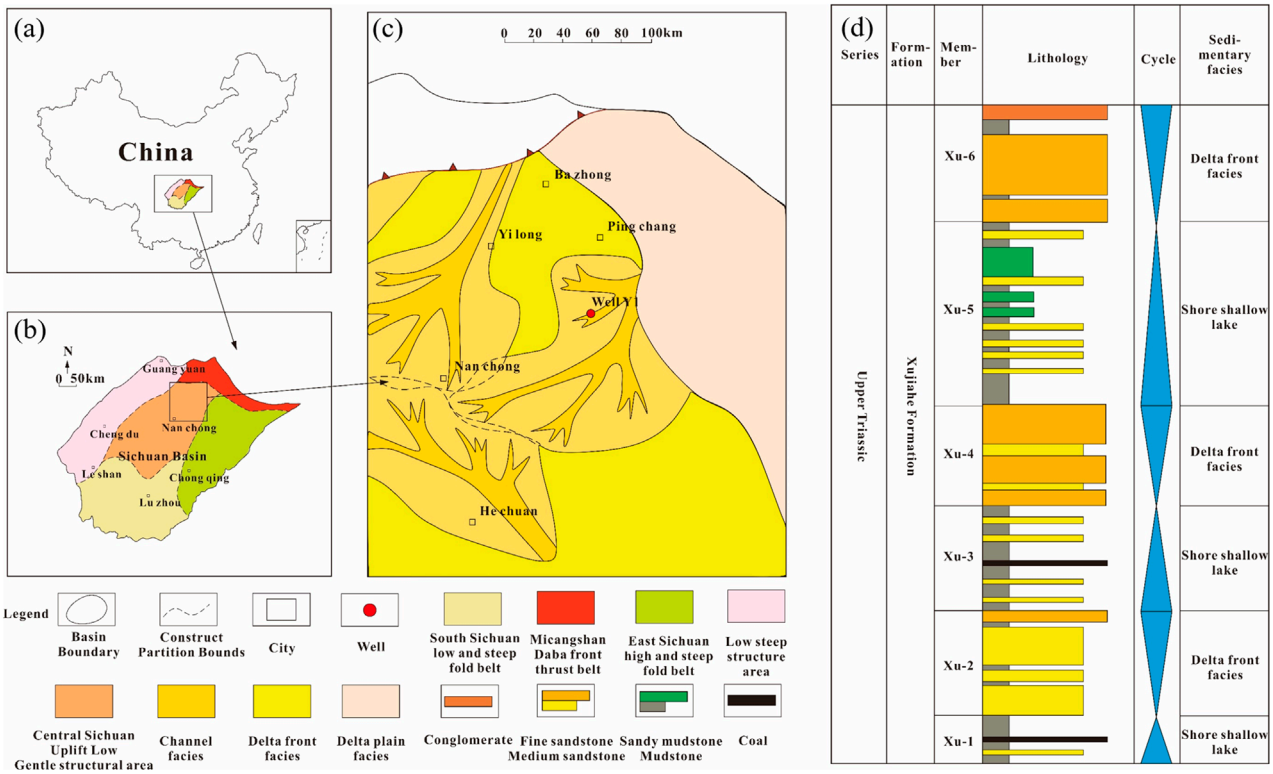

FIGURE 1
Location of the Yilong–Pingchang block and the distribution of Y1 well sites in the northeastern Sichuan Basin, South China. **(a)** Map of china; **(b)** Map of Sichuan Basin; **(c)** Sedimentary map of the Xujiahe Formation; **(d)** Composite histogram of the Xujiahe Formation.

evaluation. The porosity usually represents the ability of rocks to store oil and gas, and the permeability often represents the fluid migration ability of rocks. A total of 114 samples were prepared to measure the porosity and permeability across different sedimentary facies in the study area. Several data points were generated by the Keyuan Engineering Technology Testing Center of Sichuan Province. The porosity and permeability were analyzed via the helium method and Darcy equation according to the Chinese Oil and Gas Industry Standard (GB/T) 29172-2012. Before the experiments, residual oil was first removed from the tight sandstone samples. The porosity can be obtained based on the helium expansion, and the permeability can be accurately obtained via a bubble flowmeter.

3.2.2 Casting thin sections and scanning electron microscopy (SEM) observations

A total of 80 samples were prepared to observe the minerals, pore types, and diagenesis characteristics by petrographic microscopy that covered different sedimentary facies in the Xujiahe Formation. A total of 44 tight sandstone samples were prepared to observe the pore types and sizes (the observation accuracy was 100–1,000 nm). The samples were analyzed by using an FEI Quanta 250 FE SEM scanning electron microscope at 25°C and a relative humidity of 60% according to the GB/T18395-2001 standard for SEM. The experiment was completed at the Keyuan Engineering Technology Testing Center of Sichuan Province.

3.2.3 Cathodoluminescence (CL) observations

A total of 20 samples were prepared to reveal the minerals and diagenesis characteristics via CL observations. CL analyses were performed on an ELM3R2 L cathodoluminescence instrument at the Keyuan Engineering Technology Testing Center of Sichuan Province according to the SY/T5916-94 standard. The beam voltage was 10 kV, and the beam current was 300 μA.

3.2.4 Mercury injection capillary pressure (MICP) measurements

Mercury injection capillary pressure measurements of 114 tight sandstone samples were carried out following the SY/T 5346-2005 standard. The samples were measured at a temperature of 25°C, humidity of 20%, and at atmospheric pressure via an Autopore IV 9505 pore analyzer. Mercury intrusion/extrusion curves were obtained for every sample at pressure intervals of 0.0138–227.5269 MPa, corresponding to pore radii ranging from 0.0032 to 1,000 μm. The experiment was carried out at the Keyuan Engineering Technology Testing Center of Sichuan Province.

4 Results

4.1 Petrology and physical properties

The lithologies of the Xujiahe Formation were classified according to their mineral compositions. The mineral triangle

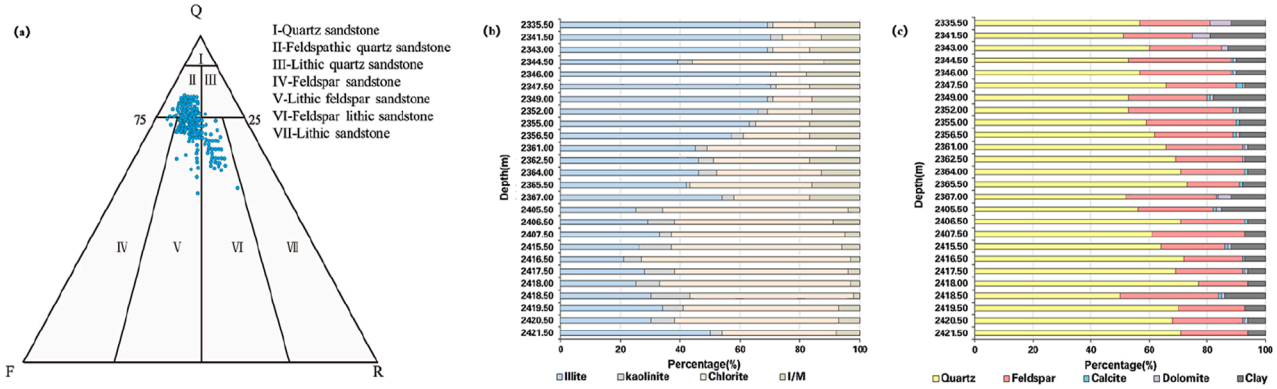

FIGURE 2
Identification of the rock types in the northeastern Sichuan Basin, South China. **(a)** Rock types of Xujiahe; **(b)** Clay composition of the Xujiahe; **(c)** Rock mineralogical composition of the Xujiahe.

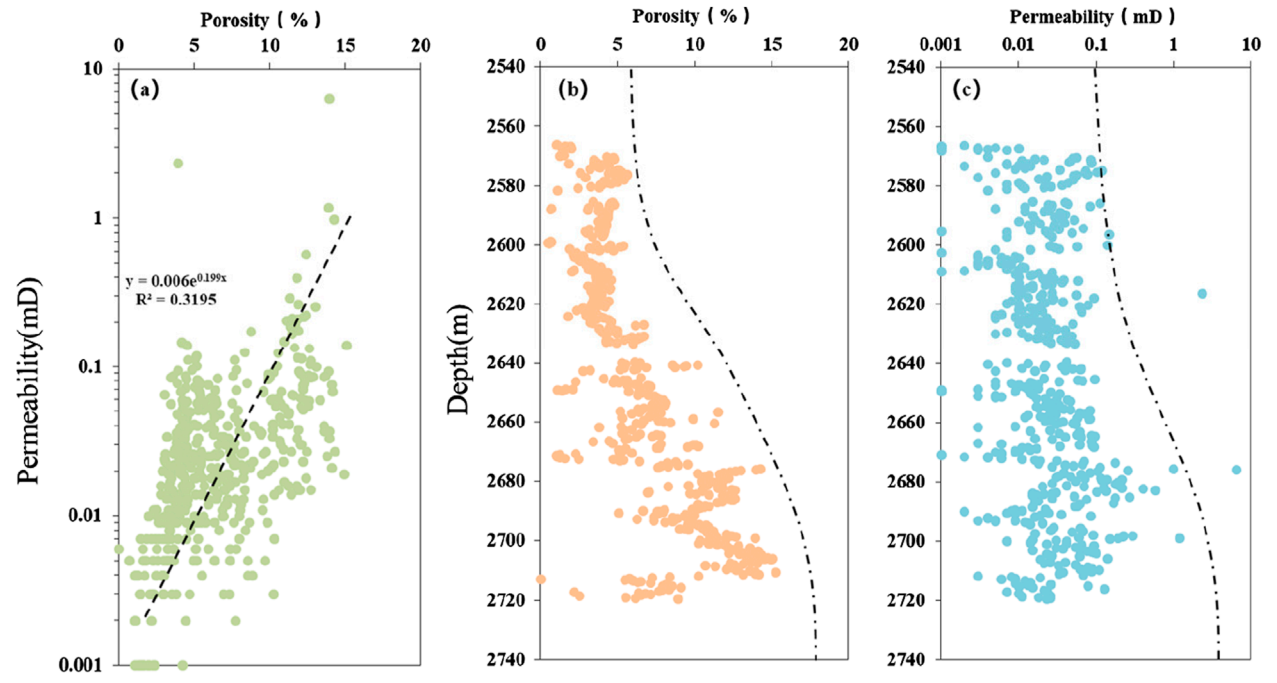

FIGURE 3
Distribution of the porosity and permeability of reservoirs in Xujiahe Formation. **(a)** Reservoir Physical Characteristics; **(b)** Relationship between porosity and depth; **(c)** Relationship between permeability and depth.

diagram and core observation results revealed that the Xu-2 member is dominated by feldspathic quartz sandstone, lithic feldspar sandstone, and feldspar lithic sandstone (Figure 2a). This clay mineral is dominated by illite (Figure 2b) and the rock-forming mineral is dominated by quartz (Figure 2c).

The tight sandstone reservoirs in the Xu-2 member in the northeastern Sichuan Basin demonstrate poor physical properties (Figure 3a), with porosities ranging from 0.7% to 15.2%, mostly less than 10% (Figure 3b). The permeability ranges from 0.0002 to 6.3 mD, mostly less than 0.1 mD (Figure 3c). However, the porosity and permeability of the Xu-2 member are highly heterogeneous. This porosity and permeability tend to increase with depth, and this porosity maximum increases from 6.7% to 15.2%.

4.2 Pore types of tight sandstone reservoirs

Developed by Loucks et al. (2012) and Nelson (2009), the classification scheme for tight reservoirs includes the following three categories: (1) organic matter (OM) pores, (2) intraparticle pores (pores within a mineral grain) (IntraP), and (3) interparticle pores

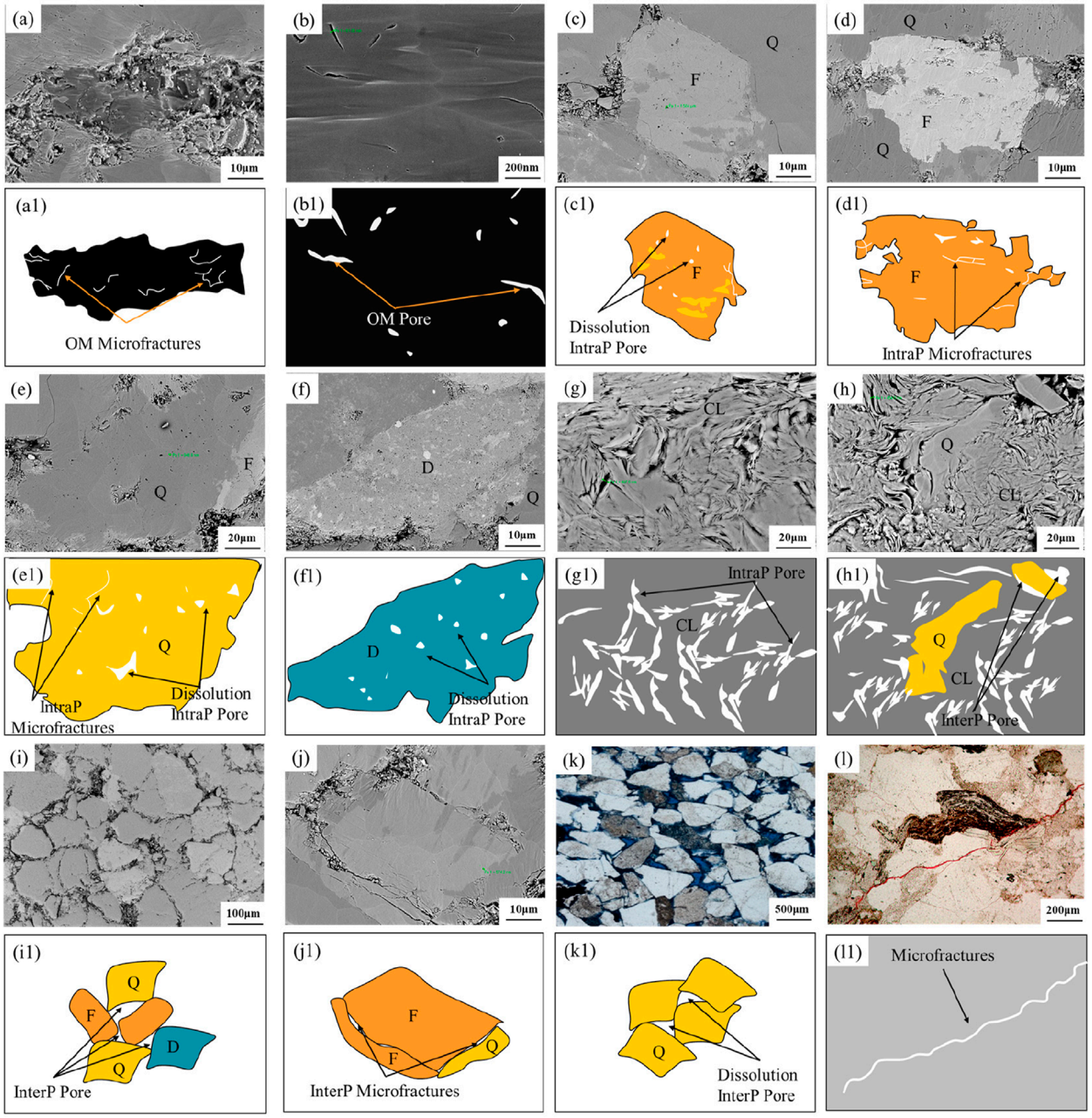

FIGURE 4
Pore types of tight sandstone reservoirs in Xujiahe Formation. **(a)** Y1 well: 2,408.5 m; **(b)** Y1 well 2,408.5 m; **(c)** Y1 well: 2,352.1 m; **(d)** Y1 well: 2,337.2 m; **(e)** Y1 well: 2,367.6 m; **(f)** Y1 well: 2,352.1 m; **(g)** Y1 well: 2,352.1 m; **(h)** Y1 well: 2,408.5 m; **(i)** Y1 well: 2,337.2 m; **(j)** Y1 well: 2,416.5 m; **(k)** Y6 well: 2,596.5 m; **(l)** Y1 well: 2,338.3 m. Q, quartz; F, feldspar; D, debris; OM, organic matter; CL, clay mineral; OM, organic matter; InterP pores, interparticle pores; IntraP pores, intraparticle pores. **(a1)** Modeling diagrams of OM Microfractures; **(b1)** Modeling diagrams of OM pores; **(c1)** Modeling diagrams of dissolution IntraP pores; **(d1)** Modeling diagrams of IntraP Microfractures; **(e1)** Modeling diagrams of quartz dissolution IntraP pores; **(f1)** Modeling diagrams of dolomite dissolution IntraP pores; **(g1)** Modeling diagrams of clay IntraP pores; **(h1)** Modeling diagrams of InterP pores; **(i1)** Model diagram of InterP pores between clastic minerals; **(j1)** Model diagram of InterP Microfractures between clastic minerals; **(k1)** Model diagram of dissolution InterP pore between clastic minerals; **(l1)** Model diagram of Microfractures.

(pores between mineral grains) (InterP). Based on this classification scheme, this study analyzed and classified the pore types of the tight sandstone samples in the Xujiahe Formation via SEM and thin sections. OM pores, mineral IntraP pores, particle InterP pores, and microfractures were found in the samples.

For hydrocarbon source rocks, convoluted OM pores, spongy OM pores, coated OM pores, and shrinkage OM pores are often found. The convoluted OM pores formed between kerogen, which is common in the hydrocarbon source rock samples obtained from the study area (Figures 4a,a1). However, OM microfractures were

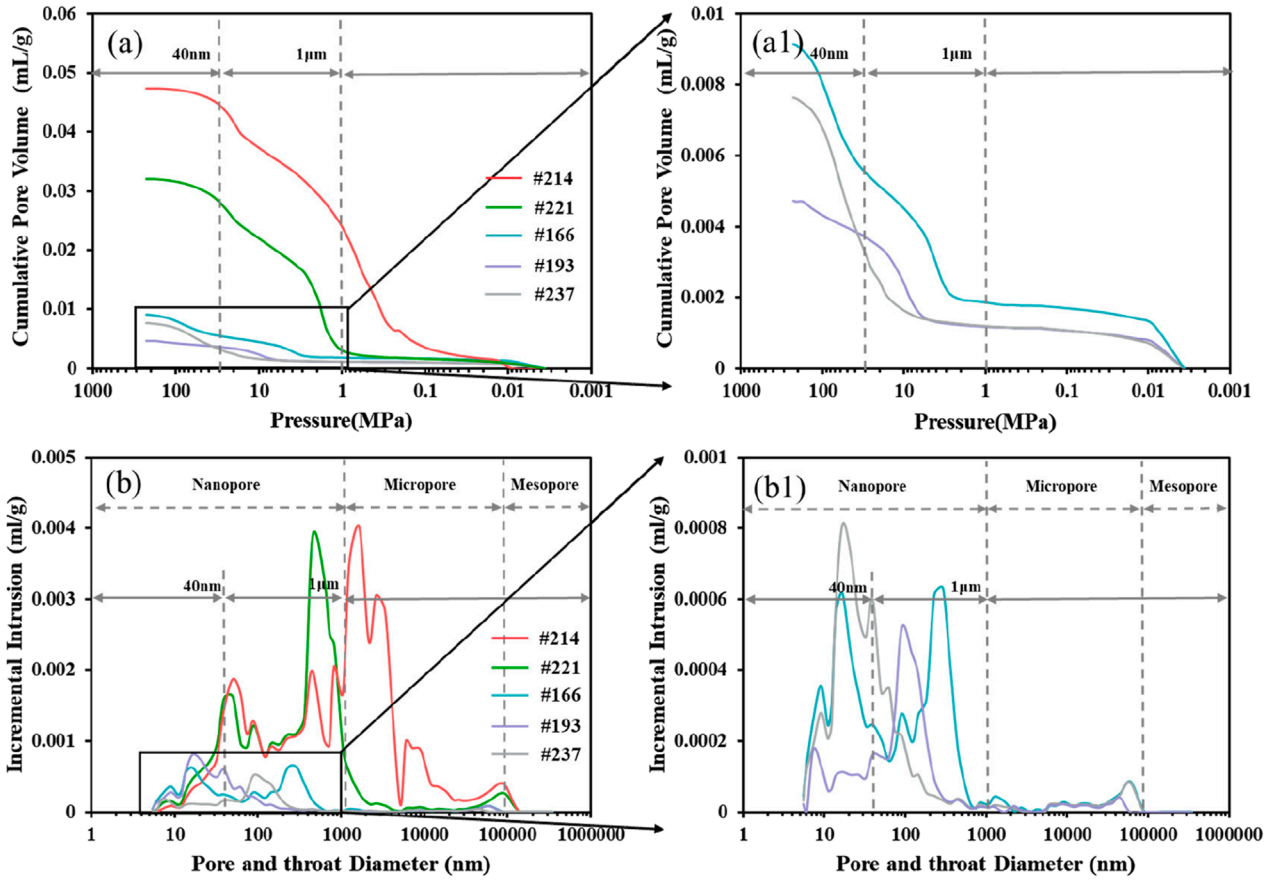

FIGURE 5
Mercury intrusion curves and pore–throat size distribution of typical tight sandstone samples. #214 = type A, #221 = type B, #166 = type C, #193 = type D, and #237 = type E. **(a)** Pressure versus pore volume graph; **(a1)** Pressure vs. pore volume plots for samples #166, #193, and #237; **(b)** Pore and throat distribution map; **(b1)** Distribution of pore throats of samples #166, #193 and #237.

TABLE 1 Basic pore–throat information of samples from Xujiahe Formation.

Sample	Porosity (%)	Permeability (mD)	Percentage of pore space			Reservoir type
			P1 (%)	P2 (%)	P3 (%)	
#214	11.30	1.4626	5.37	40.78	53.85	A
#221	7.51	0.0122	11.18	76.64	12.17	B
#166	2.64	0.0009	20.71	54.08	25.21	C
#193	2.19	0.0005	38.81	40.56	20.63	D
#237	1.71	0.0006	55.49	28.63	15.88	E

found in the samples (Figures 4b,b1), and previous studies have demonstrated that these OM microfractures are usually created during sample preparation. Therefore, the OM microfractures may not have developed in the subsurface.

For tight reservoirs, six different inorganic mineral pore types, namely intraparticle pores within clay, quartz, and feldspar mineral grains; dissolution intraparticle pores of rigid mineral grains (quartz and feldspar) (Figures 4c,c1) and debris compositions; interparticle pores between rigid mineral particles (quartz and feldspar) and debris (Figures 4d,d1); interparticle microfractures between rigid mineral particles (quartz and feldspar); dissolution interparticle pores between rigid mineral particles (Figures 4e,el); and thin-section microfractures, were identified via SEM and casting thin sections in the tight sandstone samples from the

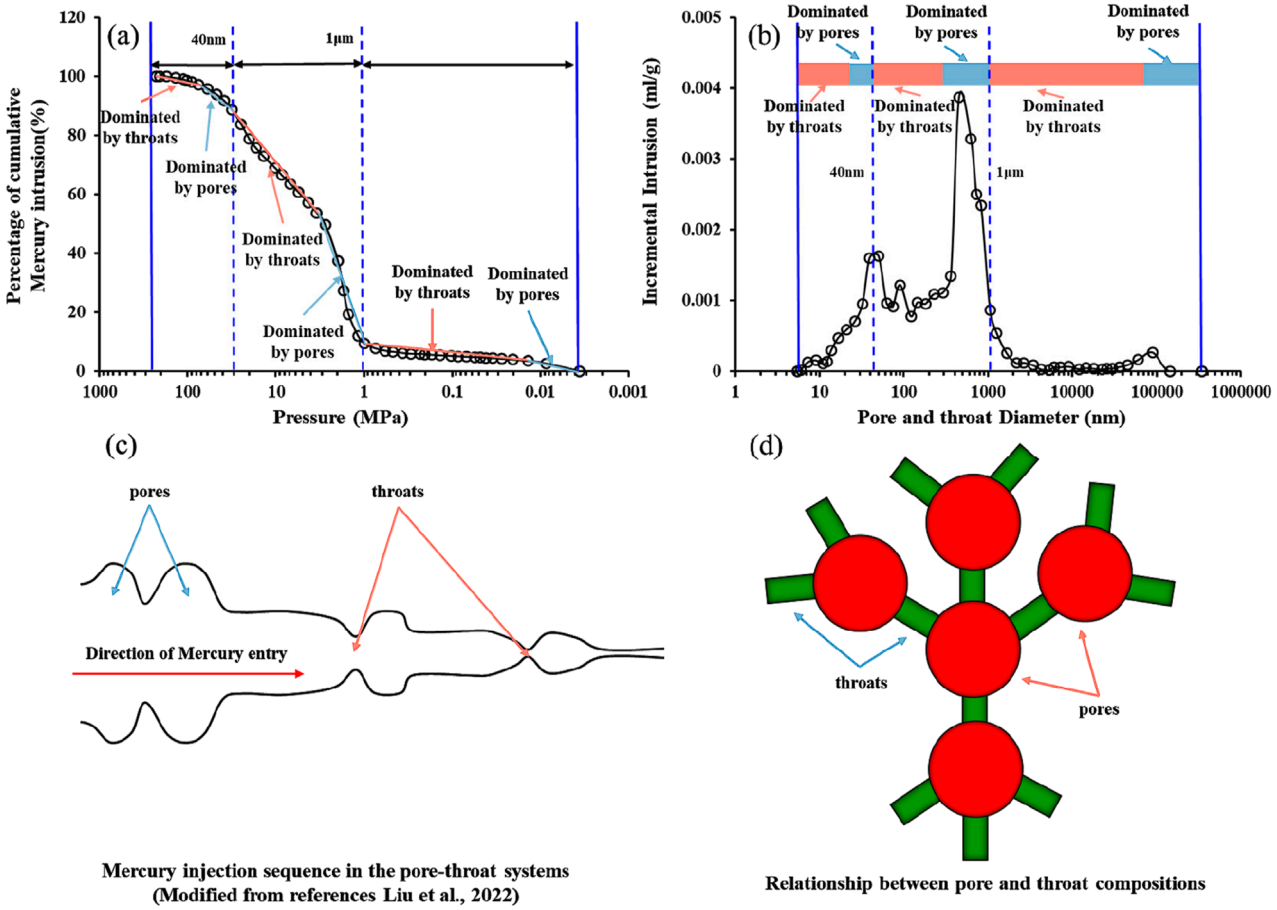

FIGURE 6
Classification of the pores–throats and relationship between pore and throat compositions. **(a)** Pressure and saturation distribution graph; **(b)** Pore and throat diameter distribution; **(c)** Mercury entry modeling diagram; **(d)** Model diagram of the composition of the pore and throat.

study area. The mineral types were effectively identified via X-ray EDS mapping and casting thin sections, and the InterP pores and dissolution InterP pores (Figures 4f,f1) were the most important pore types among the inorganic mineral pores of the study area. Primary InterP pores (Figures 4g,g1,h,h1) developed predominantly between quartz, feldspar, and illite particles (Figures 4i,i1), and dissolution InterP pores (Figures 4k,k1) and InterP microfractures (Figures 4j,j1) developed predominantly between rigid mineral particles. These pores are generally irregular in shape and range in size from a few to tens of micrometers. Therefore, the InterP pores are usually at the micrometer scale in the study area. In addition, clay intraporous pores can also be found in the study area; they are usually narrow in shape due to mechanical compaction and mineral diagenesis (Figures 4g,h). The dissolution pores of the tight sandstone are mainly subdivided into rigid mineral dissolved IntraP pores and debris dissolved IntraP pores. These pores are usually developed by quartz grain dissolution, feldspar grain dissolution, and partial debris dissolution (Figures 4k,k1). Many microfractures can be observed in the samples (Figure 4l), but it is difficult to determine whether these microfractures are still present in the subsurface. The dissolution IntraP pores have sub-rounded or sub-angular shapes, with some pores at the nanometer scale. Therefore, InterP pores and InterP dissolution pores were the most dominant and important pore types in the study area, followed by IntraP pores and IntraP dissolution pores.

4.3 Characteristics of mercury intrusion curves and pore–throat size distributions

MICP is commonly applied in the pore classification of reservoirs (Shi et al., 2019; Zhang et al., 2019), in which parameters such as mercury intrusion curves and pore–throat sizes are common indicators. The Xujiahe tight sandstone reservoirs can be divided into five types based on their mercury intrusion curve characteristics (Figures 5a,a1). In addition, to visually compare the pore distribution characteristics of different tight samples, a pore structure classification method was proposed by Liu to classify the pores into P1 (1–40 nm), P2 (40 nm–1 μm), and P3 (1–100 μm) (Figures 5b,b1). Type A reservoirs have low mercury intrusion pressure (approximately 0.2 MPa), and the percentage of microscale pores (P3) exceeds 50% (Table 1), indicating that these reservoirs have large pore–throats such as InterP pores and InterP dissolution pores. Type B reservoirs also have low mercury intrusion pressure (approximately 1 MPa), the early mercury injection rates are observed to be fast, and the percentage of

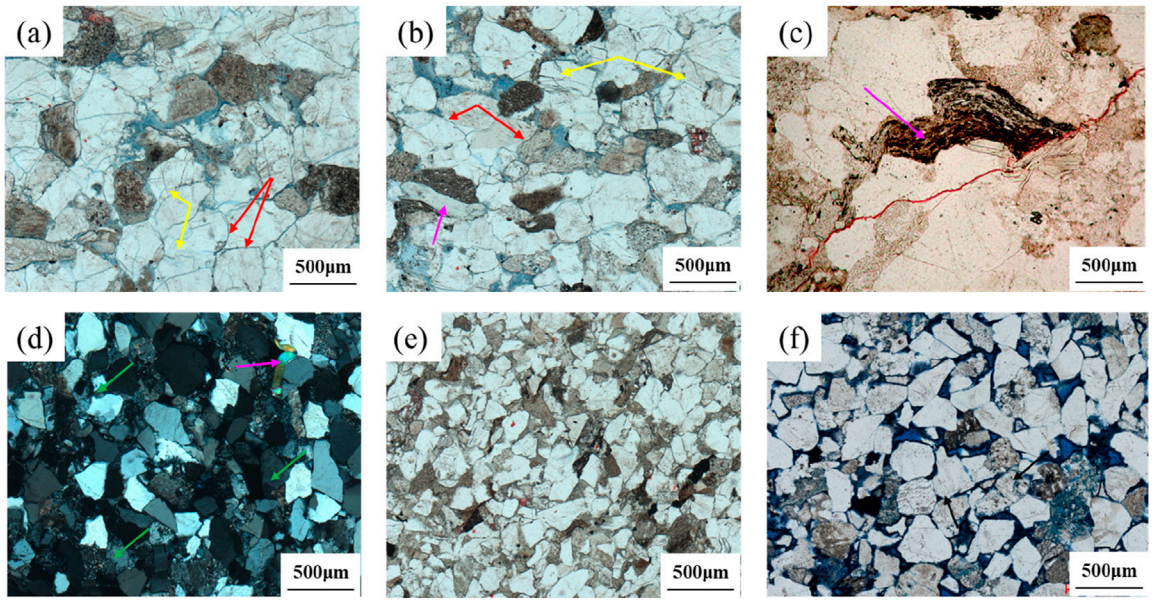

FIGURE 7
Compaction characteristics of the tight sandstone of the Xujiahe Formation. **(a)** Y1 well: 2,416.5 m; **(b)** Y1 well: 2,337.2 m; **(c)** Y1 well: 2,338.3 m; **(d)** Y6 well: 2,590.4 m; **(e)** Y1 well: 2,341.5 m; **(f)** Y6 well: 2,596.6 m. Red arrows represent concave–convex contact, yellow arrows represent fractures, green arrows represent sutured contacts, and pink arrows represent plastic grains deformation.

microscale pores (P3) is 12.17% (Table 1). Type C reservoirs have visually high mercury intrusion pressures (approximately 3 MPa), and the mercury intrusion volumes are significantly smaller than those of the type A and B reservoirs, indicating that the reservoir physical properties are poor and that the percentage of microscale pores (P3) is 20.63% (Table 1). Type D reservoirs have higher mercury intrusion pressure (approximately 8 MPa) than the type C reservoirs, and the percentage of microscale pores (P3) is 25.21% (Table 1). Type E reservoirs have the highest mercury intrusion pressure (approximately 11 MPa), the quality of these reservoirs is the worst, and the pore space is dominated by P1 (Table 1), indicating that the reservoirs have small pore–throats, such as clay IntraP pores.

4.4 Relationships between pore and throat compositions

The mercury injection capillary pressure is a quantitative evaluation method for determining pore structures of tight reservoirs (Zou et al., 2012; Dai et al., 2024). With increasing mercury injection pressure, mercury enters pores and throats of different sizes (mercury enters the large pore–throat first, followed by the small pore–throat) (Figure 6c). In general, mercury is not a wettable fluid for rocks, and if mercury is injected into the pore space of the sample (after the removal of residual oil), mercury overcomes the capillary resistance of the pore–throats. Therefore, when the mercury injection pressure and the capillary resistance of the pore–throat of a rock sample are balanced, the mercury injection pressure and the volume of mercury entering the rock sample under these pressure conditions can be measured; thus, a mercury injection curve can be obtained. Previous studies have shown that the contributions of pores and throats can be revealed based on the slope of the mercury injection curve. The low-slope part is dominated by the throats (which need to overcome the capillary pressure, resulting in a slow mercury feed rate), and the high-slope part is dominated by the pores (Figure 6a). After the contributions of the pores and throats are revealed, the characteristics of the pore–throat compositions (including large pore–small throat, short catheter, and tree-shaped network) can be effectively obtained.

By incorporating sample #211 in from well Y1 as an example, the results indicated that mercury rapidly accesses the pore-dominated space at the beginning and then enters the throat-dominated space. The sample is dominated by P2 pore space, and the pores and pore–throats are of nanoscale dimensions. Based on the contributions of pores and throats, this composition of pore–throat characteristics can be obtained, and the pore volume is clearly larger than the throat volume (Figure 6b), so the sample is dominated by a large pore–small throat composition (Figure 6d).

4.5 Reservoir diagenesis

Diagenesis events can be divided into four types for the tight sandstone reservoirs of the Xujiahe Formation, including compaction, cementation, and dissolution. These factors have different effects on the reservoir quality of tight sandstone.

4.5.1 Compaction

There is heavy mechanical and chemical compaction of the tight sandstone in the Xujiahe Formation. For mechanical compaction,

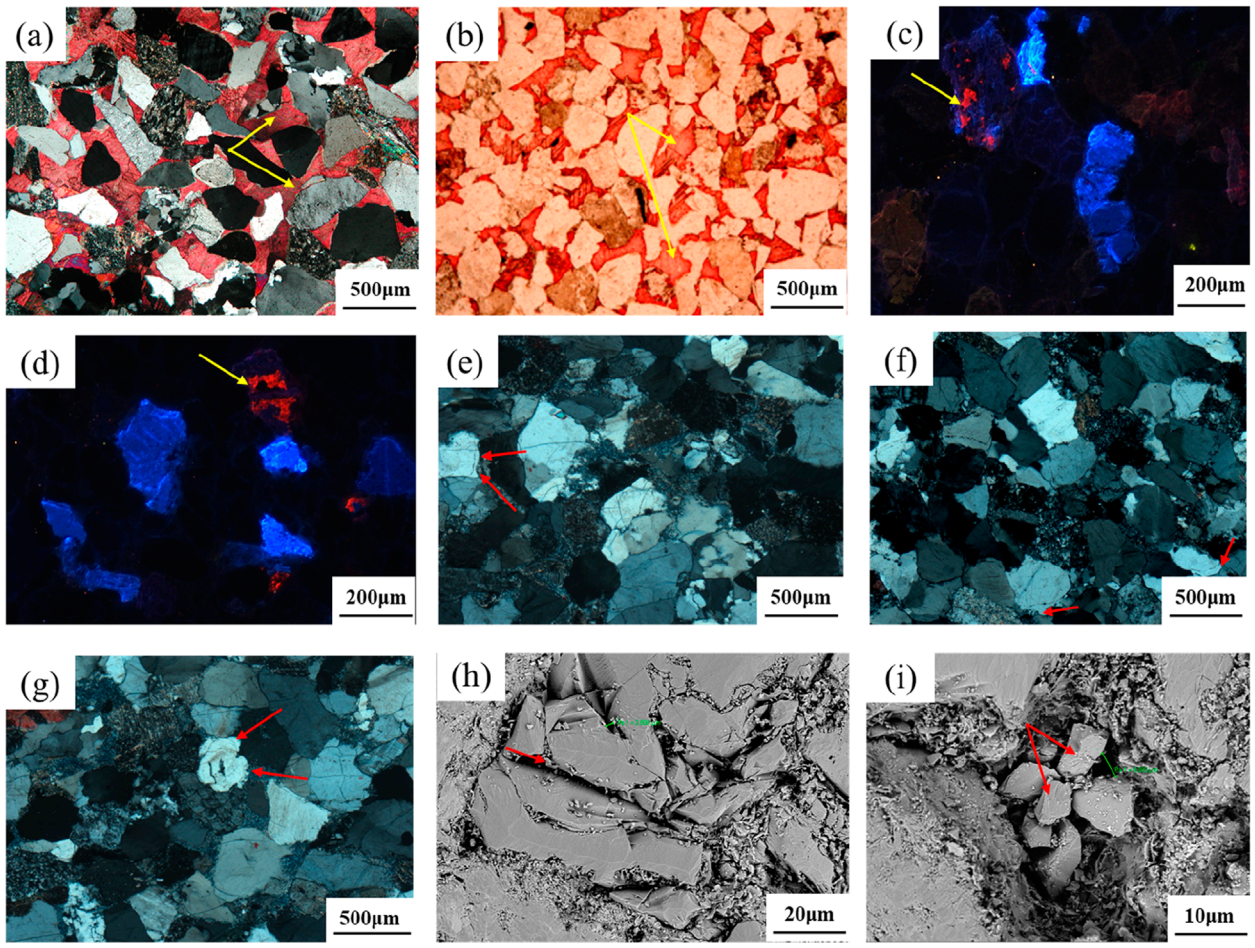

FIGURE 8
Cementation characteristics of the tight sandstone of the Xujiahe Formation. **(a)** Y1 well: 2,416.5 m; **(b)** Y1 well: 2,337.2 m; **(c)** Y1 well: 2,338.3 m; **(d)** Y6 well: 2,590.4 m; **(e)** Y6 well: 2,593.5 m; **(f)** Y6 well: 2,596.6 m; **(g)** Y6 well: 2,590.4 m; **(h)** Y1 well: 2,340.5 m; **(i)** Y1 well: 2,342.6 m. Yellow arrows represent calcite cementation, and red arrows represent quartz overgrowth.

this view can be suggested by several typical phenomena, such as concave-convex contacts between quartz particles (Figures 7a,b). In addition, the deformation of some plastic grains is also typical evidence of mechanical compaction (Figures 7c,d). Direct evidence of mechanical compaction consists of the fracturing of quartz particles (Figures 7a,b). For chemical compaction, the concave–convex and sutured contacts (generated by pressure dissolution) of some plastic grains are typical evidence of chemical compaction (Figures 7d,e). Moreover, this phenomenon revealed that there are obvious InterP pores between the particles wrapped by chlorite (Figure 7f), indicating that chlorite effectively attenuates compaction.

4.5.2 Calcite and quartz cementation

There are different cementation events (calcite and quartz cementation) that are reflected by CL and thin sections in the tight sandstone reservoirs of the Xujiahe Formation. The calcite cementation events in the Xujiahe Formation are dominated by two periods of calcite cementation. In general, first-generation calcite developed on the edge of clastic particles with dark red light (Figures 8a,b). It is very commonly believed that first-generation calcite cements formed before or during compaction. The subsequent formation of calcite cements emits bright red light and fills the InterP pores or pores created by feldspar dissolution (Figures 8c,d). The pore–throat systems of tight sandstone reservoirs were heavily destroyed by calcite cementation. In addition, quartz overgrowths play an important role in cementation events. They are usually accompanied by sutured quartz grain contacts (Figures 8e,g). SEM observations revealed that some InterP pores were cemented with quartz (Figures 8h,i).

4.5.3 Clay minerals

The clay minerals of the tight sandstone reservoir in the Xujiahe Formation, which primarily consist of chlorite, illite, mixed-layer illite/smectite, and minor kaolinite, were identified via XRD (Figure 9a). Clay minerals occur mainly as cementation-compositions, with nested aggregates filling in secondary IntraP dissolved pores and non-netted aggregates filling in InterP pores (Figures 9b,c). Illite and chlorite are found in InterP pores in the form of assemblages (Figures 9d,e).

The formation of clay minerals is linked, and chemical reactions occur between the particles. Authigenic kaolinite can be generated by the dissolution of albite ($CaAlSi_2SO_8$)

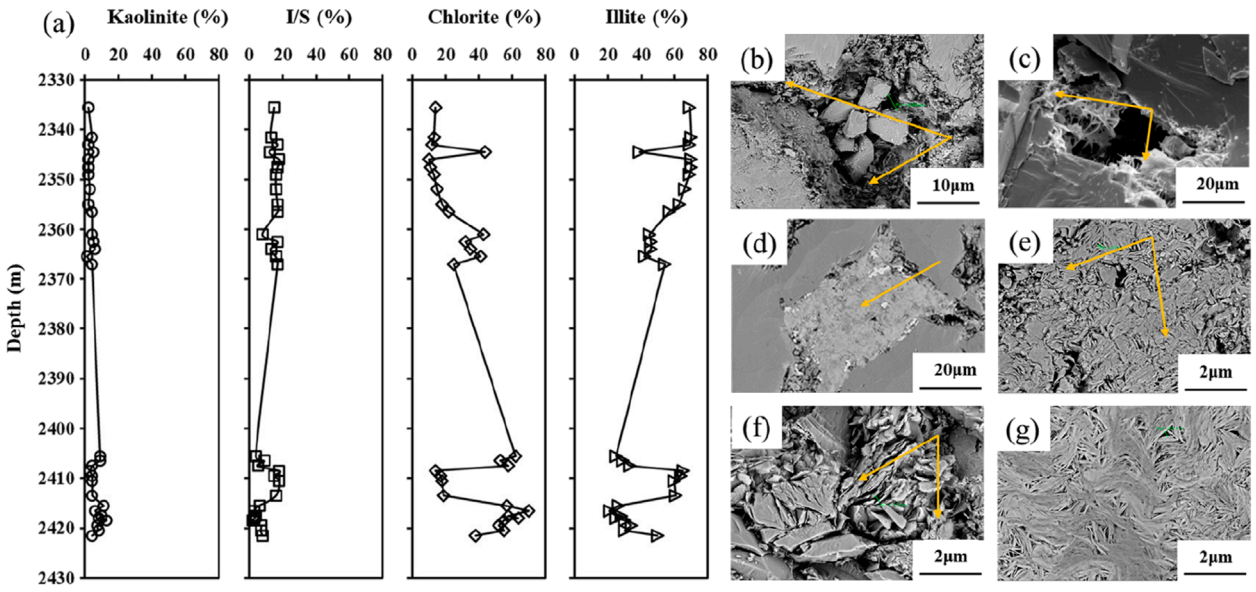

FIGURE 9
Cementation characteristics of the tight sandstone of the Xujiahe Formation. **(a)** Relationship between clay minerals and depth; **(b)** Y1 well: 2,337.2 m; **(c)** Y1 well: 2,416.5 m; **(d)** Y1 well: 2,420.6 m; **(e)** Y1 well: 2,408.5 m; **(f)** Y1 well: 2,367.6 m; **(g)** Y1 well: 2,352.1 m.

and anorthite (2 $NaAlSi_3SO_8$) during early diagenesis, and the related chemical equations are as follows (Equations 1, 2). K^+ is required in the conversion of smectite ($K\ AlSi_3SO_8$) to illite ($K_{5.5}Mg_2Fe_{1.5}Al_{22}Si_{35}O_{100}(OH)_2$) (Equation 3); in the presence of acidic fluids, Na^+ is consumed and converted to K^+ (Equation 4), which provides the source of K^+ for the formation of illite. The morphology of chlorite primarily includes rims (Figure 9f) and foliated shapes (Figure 9g) in the tight sandstone reservoir. The InterP pores can be effectively preserved between chlorites, indicating that chlorite formed during or after the densification of the sandstones in the Xujiahe Formation. Chlorite rims can be generated in iron- and magnesium-rich diagenetic environments.

$$CaAlSi_2SO_8 + 2H^+ + H_2O = Al_2Si_2O_5(OH)_4 + 4SiO_2 + Ca^{2+}. \quad (1)$$

$$2NaAlSi_3SO_8 + 2H^+ + H_2O = Al_2SiO_5(OH)_4 + 4SiO_2 + Na^{2+}. \quad (2)$$

$$4.5K^+ + 8Al^+ + KNaCa_2Mg_4Fe_4Al_{14}Si_{38}O_{100}(OH)_2 = K_{5.5}Mg_2Fe_{1.5}Al_{22}Si_{35}O_{100}(OH)_2 + Na^{2+} + 2Ca^{2+} + 2.5Fe^{3+} + 2Mg^{2+} + 3Si^{4+}. \quad (3)$$

$$K\ AlSi_3SO_8 + Na^+ + H_2O = NaAlSi_3O_8 + K^+. \quad (4)$$

4.5.4 Dissolution

Dissolution pores, as an important pore type in the Xujiahe Formation, are usually developed by the dissolution of anorthite, potassium feldspar, and volcanic rock fragments (Figures 10a–i). Dissolution plays an important role in improving the reservoir properties of the tight sandstone in the Xujiahe Formation. Dissolution is the solution of debris particles, heterogeneous bases, and cement, which is very favorable for the formation of reservoirs and is the most important constructive rock-forming action in this area.

5 Discussion

5.1 Classification of the pore–throat systems of a tight sandstone reservoir

This classification is very closely linked to the pore–throat systems and pore types of tight sandstone reservoirs (Liu L. et al., 2024; Li W. et al., 2024). When tight sandstone reservoirs are dominated by a class of pores and have a certain permeability, a complete pore–throat system of pores and their adjacent throats is composed. If sandstone reservoirs are clearly dominated by a certain type of pore system, this reservoir is defined as a single pore–throat system, such as an intergranular pore–throat system. If the reservoirs develop multiple pore–throat systems, the reservoirs are defined as a mixed pore–throat system, such as intergranular-dissolved-intercrystalline mixed pore–throat systems. Based on cast thin sections and SEM experiments, the pore–throat systems of this tight sandstone can be effectively identified. The results revealed three types of pore–throat systems, namely intergranular pore–throat systems, intergranular-dissolved mixed pore–throat systems, and dissolved-intercrystalline pore–throat systems.

The intergranular pore–throat system primarily features many residual intergranular pores (Figures 11a,b). The gaps between fragment particles form pores, and the points of particle contact form pore–throats, resulting in good connectivity. This system is mainly distributed in class A reservoir layers. The dissolution and intergranular mixed pore–throat system is characterized

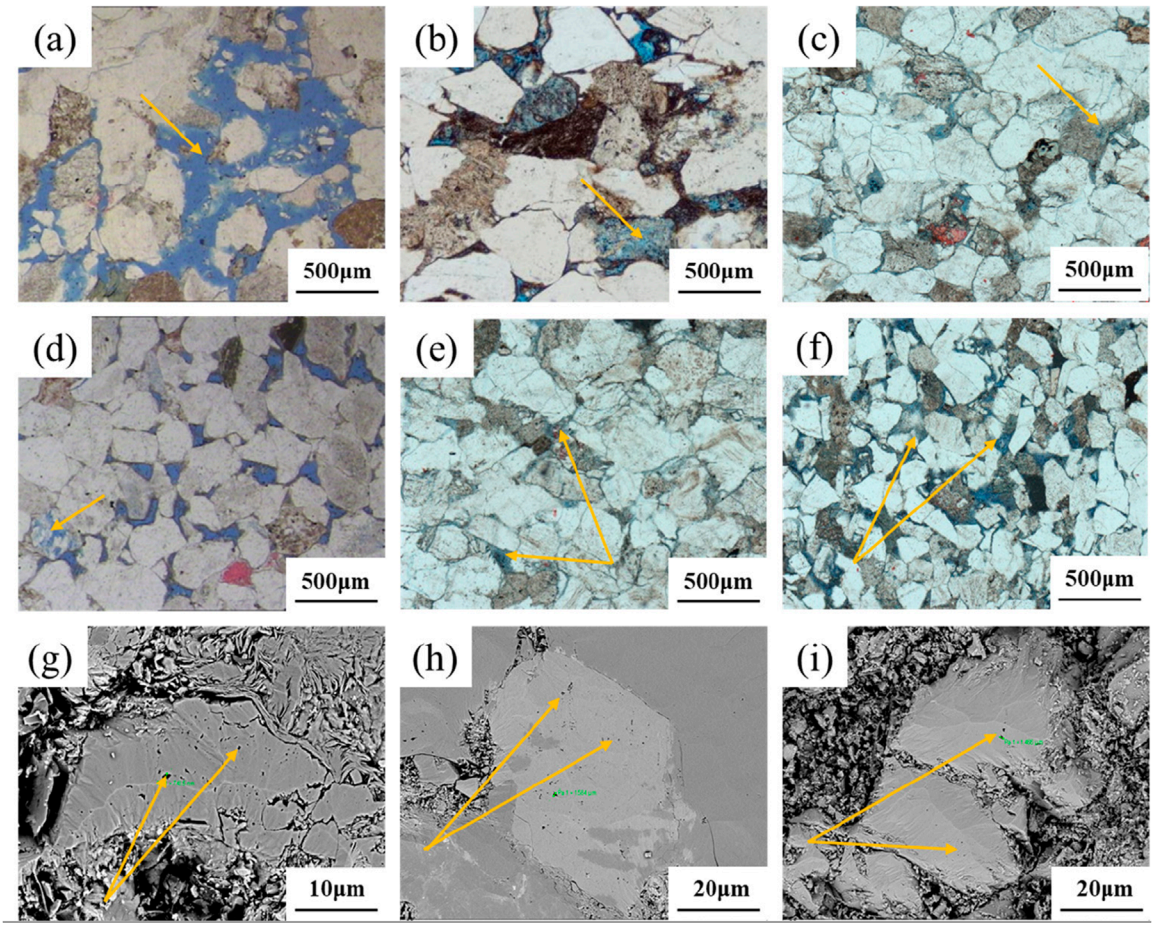

FIGURE 10
Cementation characteristics of the tight sandstone of the Xujiahe Formation. **(a)** Y6 well: 2,590.4 m; **(b)** Y6 well: 2,596.5 m; **(c)** Y1 well: 2,338.3 m; **(d)** Y6 well: 2,590.4 m; **(e)** Y1 well: 2,416.5 m; **(f)** Y1 well: 2,338.3 m; **(g)** Y1 well: 2,367.6 m; **(h)** Y1 well: 2,352.1 m; **(i)** Y1 well: 2,337.2 m.

by intergranular dissolution pores as the dominant pore type (Figures 11c,d), with a small number of residual intergranular pores. The intergranular dissolution pores have a honeycomb structure, with larger sections forming pores and narrower sections forming throats. The coordination number of pore–throats is high, and the dense distribution of dissolution pores demonstrates good connectivity. This type of pore system is relatively simple with good pore–throat sorting, and is it found mainly in class B and C reservoir layers. Dissolution and intracrystalline pore–throat systems are dominated by intracrystalline dissolution pores. Soluble minerals such as feldspar react with organic acids to form intracrystalline dissolution pores (Figures 11e,f). The connectivity of these dissolution pores is generally poor, and they are mainly distributed in class D and E reservoir layers.

The microscopic characteristics of reservoir layers significantly vary in pore–throat systems (Figure 12). Intergranular pore–throat systems are characterized by the broadest pore distribution, with the largest proportion of large pores (pore radii greater than 1 μm). The size of the pore–throat system is typically greater than 0.4 μm, indicating the presence of well-developed intergranular pores. The pore–throat relationship is characterized primarily by large pores with fine throats. Dissolution and intergranular mixed pore–throat systems are characterized by pore radii ranging from 0.01 to 0.1 μm, with pore–throat size generally greater than 0.15 μm. These systems indicate a gradual reduction in residual intergranular pores, with dissolution pores beginning to dominate. The pore–throat relationships consist primarily of the short conduit type. In dissolution and intracrystalline pore–throat systems, the pore radii are primarily less than 0.01 μm, and the pore–throat sizes are predominantly smaller than 0.1 μm, indicating a reduction in residual intergranular pores, with dissolution pores becoming increasingly dominant. The pore–throat relationship is characterized by a dendritic network.

5.2 Influence of diagenesis on pore–throat systems

The Xujiahe Formation experienced three types of diagenesis: compaction, cementation, and dissolution. These processes influence pore–throat systems. The image processing method combined with casting thin section allows the surface porosity and cement content of intergranular porosity and dissolution porosity in the samples to be obtained. The relationship between

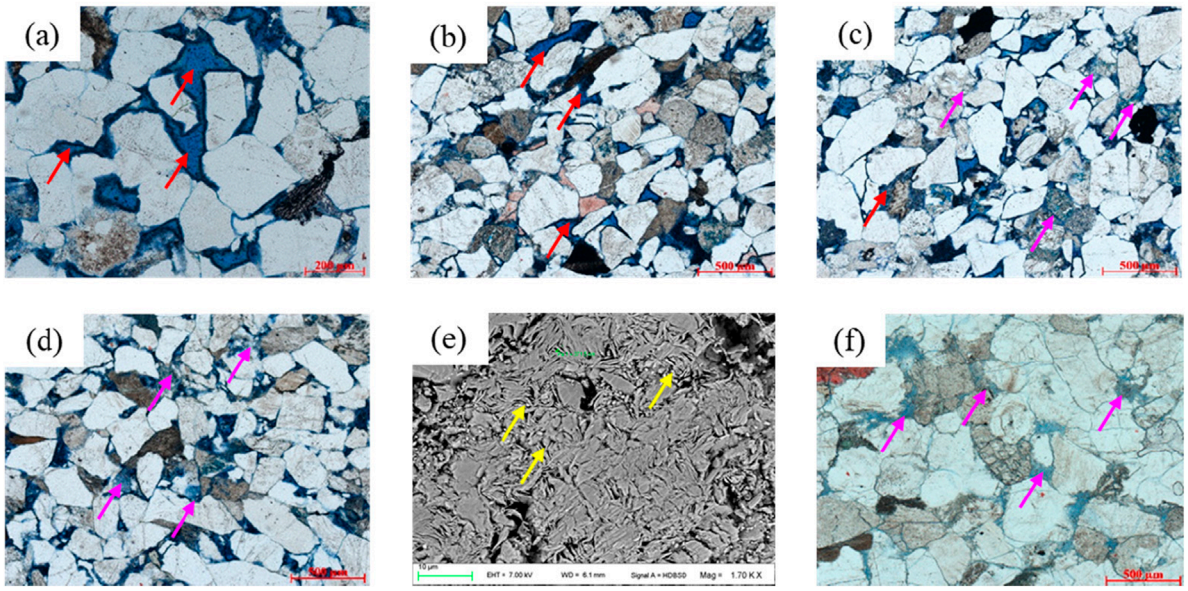

FIGURE 11
Classification of pore–throat systems in Xujiahe Formation sandstone. **(a)** Y6 well: 2,590.4 m; **(b)** Y6 well: 2,596.5 m; **(c)** Y6 well: 2,603.5 m; **(d)** Y6 well: 2,600.6 m; **(e)** Y1 well: 2,416.5 m; **(f)** Y1 well: 2,416.5 m. Red arrows represent InterP pores, pink arrows represent dissolution pores, and yellow arrows represent IntraP pores.

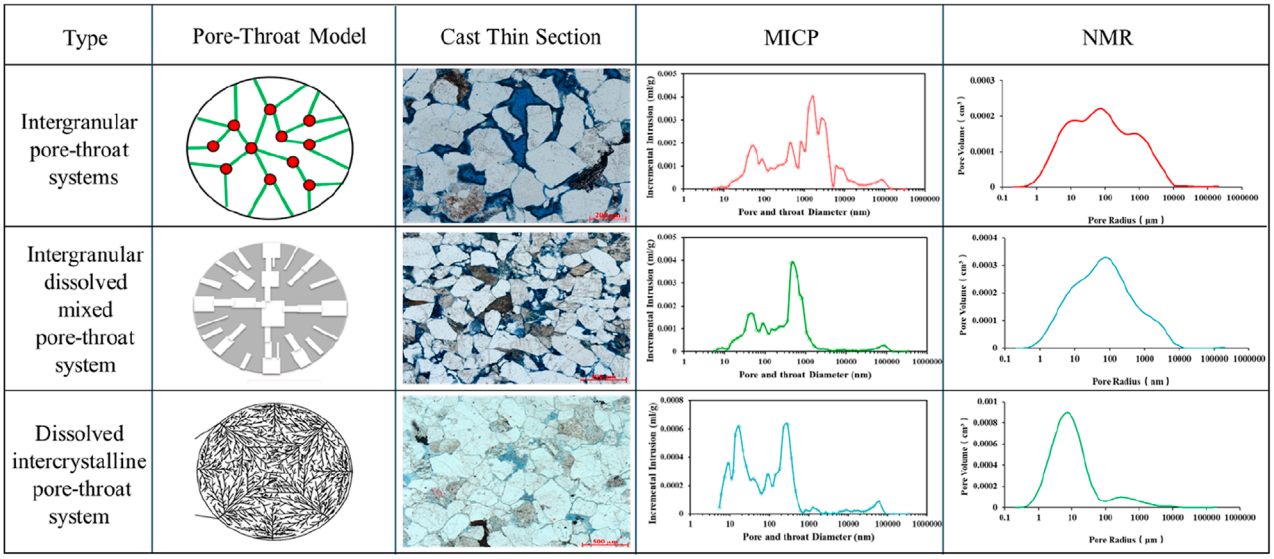

FIGURE 12
Classification of pore–throat systems in Xujiahe Formation.

surface porosity and effective porosity can be used to determine the intergranular porosity and dissolution porosity. The intergranular porosity and dissolution porosity can be converted to obtain the original porosity by combining the calculation of the rock grain sizes. This can be used to deduce the effects of different diagenetic effects on porosity (e.g., compaction porosity reduction, dissolution porosity enhancement, and cementation porosity reduction).

The destructive effect of diagenesis has been observed on different types of pore–throat systems, with the degree of improvement varying significantly (Figure 13). Intergranular pore–throat systems, in particular, exhibit the distinctive characteristics of "weak compaction and strong dissolution." These samples have the lowest compaction pore reduction rates and the highest dissolution pore increase rates. Additionally, there is a clear positive correlation between the pore–throat

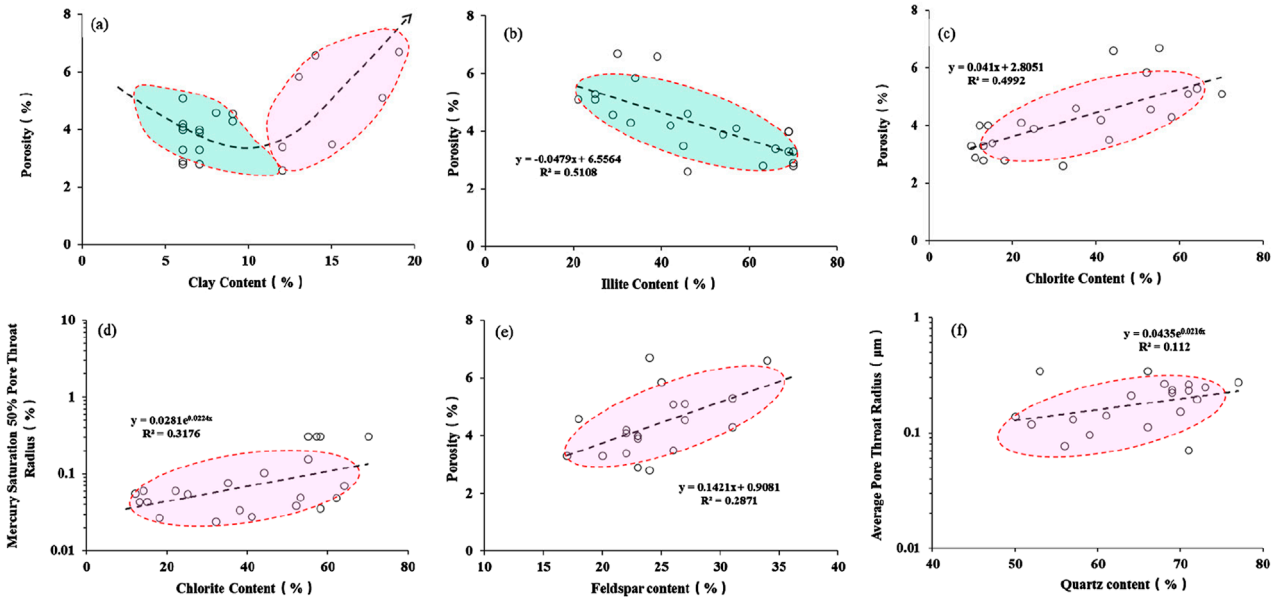

FIGURE 13
Impact of diagenesis on pore structure. **(a)** Relationship between clay content and porosity; **(b)** Relationship between illite content and porosity; **(c)** Relationship between chlorite content and porosity; **(d)** Relationship between chlorite and pore throat radius; **(e)** Relationship between feldspar content and porosity; **(f)** Relationship between quartz content and average pore throat radius.

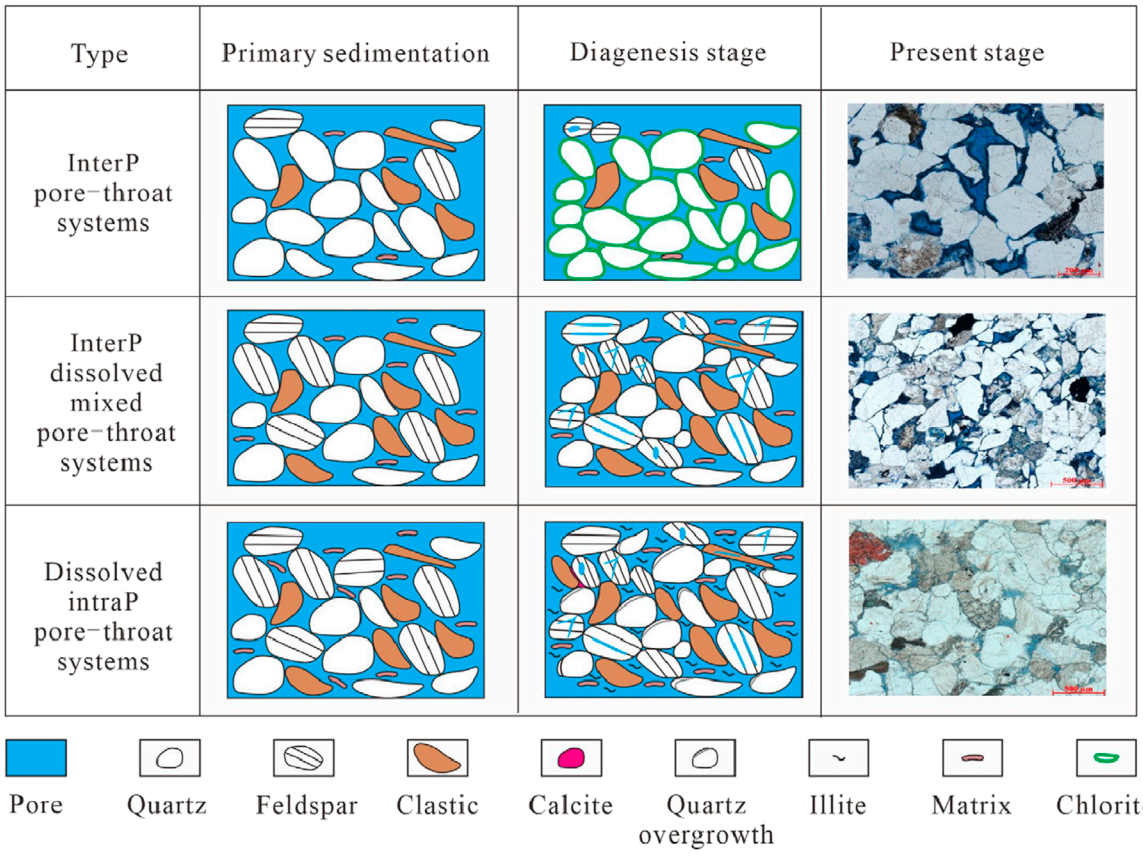

FIGURE 14
Patterns of evolution of different types of pore–throat systems.

radii, porosities, and chlorite content; this is attributable to the early hydrolysis of volcanic rock debris, which releases Fe, Mg, and other ions. These ions form chlorite films on the primary intergranular pore walls, thereby effectively inhibiting cementation. This phenomenon can be attributed to the process of early hydrolysis of volcanic clasts, which results in the release of Fe and Mg ions. These ions subsequently form chlorite films within the primary intergranular pore walls, thereby effectively inhibiting cementation and preserving a significant number of primary intergranular pores. Dissolution and intergranular mixed pore–throat systems are characterized by "strong compaction and strong dissolution." Furthermore, a positive correlation is evident between porosity and feldspar content, suggesting that feldspar particles are susceptible to dissolution by organic acids. The development of dissolution pores and dissolution joints can also enhance the storage capacity. Dissolution intergranular pore–throat systems clearly indicate "strong cementation" that is characterized by significant cementation of mud and calcium, low pore-enhancement rate due to dissolution, and compromised physical properties of the reservoir.

5.3 Reservoir genesis in different types of pore–throat systems

The combination of sedimentary environments and diagenesis controls the type of reservoir pore–throat system (Figure 14). During the Xu-2 depositional period, deltaic deposits developed in the study area, resulting in lower rock debris contents, stronger hydrodynamics, higher quartz grain contents, and greater resistance to rock compaction. This type of pore and throat system has developed mainly in distributary river channels. Moreover, moderate amounts of volcanic rock debris were present in the rocks, large amounts of chlorite film further developed, and the intergranular pores were effectively preserved. When the hydrodynamic force becomes weak, the content of the heterogeneous base in the sediment increases, the ability to resist compaction decreases, the primary intergranular pore space is destroyed, and the residual intergranular pore space develops. Meanwhile, feldspars and other minerals in the later stage are dissolved by organic acids, forming a large amount dissolved pore space, which greatly improves the physical properties of the reservoir and forms a mixed pore–throat system of intergranular and dissolved pore space. In the hydrodynamically weaker parts, the rock grain size is small, and the plastic components, such as the heterogeneous base and mudstone rock debris, increase. The early primary pores suffer considerable destruction, and the later dissolution effect is also weak. A small number of dissolution pores and clay intergranular pores have developed, forming a mixed dissolution and intergranular pore–throat system. This type of pore-throat system has mainly developed in inter-channel bays or sand barriers.

6 Conclusion

(1) The cast thin sections reveal four main types of reservoir space in the Xujiahe Formation, namely, primary intergranular pores, residual intergranular pores, dissolution pores, and intergranular pores.

(2) The pore–throat systems of this dense sandstone can be efficiently identified based on casting thin section and SEM experiments, and three types of pore–throat systems can be identified: an intergranular pore–throat system, a mixed intergranular–dissolutional pore–throat system, and a dissolution–intergranular pore–throat system. (3) The pore–throat system of the reservoir is controlled by both the sedimentary environment and diagenesis, strong hydrodynamics, high quartz grain contents, low mud and calcareous clast contents, and moderate amounts of volcanic clasts that are favorable for chlorite film formation. A large number of intergranular pores are efficiently maintained, forming an intergranular pore–throat system with the best storage conditions.

Data availability statement

The original contributions presented in the study are included in the article/supplementary material; further inquiries can be directed to the corresponding author.

Author contributions

YW: writing – original draft and writing – review and editing. XW: writing – original draft. XC: writing – original draft. XL: writing – original draft. JW: writing – original draft. XG: investigation and writing – review and editing. JP: investigation and writing – review and editing. BW: project administration, resources, and writing – review and editing. YX: project administration and writing – review and editing. HW: investigation, software, and writing – review and editing.

Funding

The author(s) declare that no financial support was received for the research and/or publication of this article.

Conflict of interest

Authors YW, XW, XC, XL, JW, XG, JP, BW, and YX were employed by the Exploration and Development Research Institute of Daqing Oilfield Company Ltd.

The remaining author declares that the research was conducted in the absence of any commercial or financial relationships that could be construed as a potential conflict of interest.

The reviewer ST declared a shared affiliation with the author HW to the handling editor at the time of review.

Generative AI statement

The author(s) declare that no Generative AI was used in the creation of this manuscript.

Publisher's note

References

Chen, X., Ji, Y., and Yang, K. (2024). Impacts of sedimentary characteristics and diagenesis on reservoir quality of the 4th member of the Upper Triassic Xujiahe formation in the western Sichuan basin, southwest China. *Mar. Petroleum Geol.* 167, 106981. doi:10.1016/j.marpetgeo.2024.106981

Dai, J., Dong, D., Ni, Y., Gong, D., Huang, S., Hong, F., et al. (2024). Distribution patterns of tight sandstone gas and shale gas. *Petroleum Explor. Dev.* 51 (4), 767–779. doi:10.1016/S1876-3804(24)60505-7

Deng, J., Liu, M., Ji, Y., Tang, D., Zeng, Q., Song, L., et al. (2022). Controlling factors of tight sandstone gas accumulation and enrichment in the slope zone of foreland basins: the Upper Triassic Xujiahe Formation in Western Sichuan Foreland Basin, China. *J. Petroleum Sci. Eng.* 214, 110474. doi:10.1016/j.petrol.2022.110474

Dong, Z., Tian, S., Xue, H., Lu, S., Liu, B., Erastova, V., et al. (2024). Analysis of pore types in lower cretaceous qingshankou shale influenced by electric heating. *Energy and Fuels* 38 (21), 20577–20590. doi:10.1021/acs.energyfuels.4c03783

Dong, Z., Tian, S., Xue, H., Lu, S., Liu, B., Erastova, V., et al. (2025). A novel method for automatic quantification of different pore types in shale based on SEM-EDS calibration. *Mar. Petroleum Geol.* 173, 107278. doi:10.1016/j.marpetgeo.2024.107278

Garcia-Hidalgo, J. F., Gil, J., Segura, M., and Dominguez, C. (2007). Internal anatomy of a mixedsiliciclastic–carbonate platform: the late cenomanian–mid turonian at the southern margin of the Spanish central system. *Sedimentology* 54 (6), 1245–1271. doi:10.1111/j.1365-3091.2007.00880.x

Guan, X., Xiao, D., Jin, H., Cui, J., Wang, M., Shao, H., et al. (2024). Classification and controlling factors of different types of pore throat in tight sandstone reservoirs based on fractal features—a case study of Xujiahe Formation in western sichuan depression. *Minerals* 15 (1), 18. doi:10.3390/min15010018

He, T., Li, W., Lu, S., Yang, E., Jing, T., Ying, J. F., et al. (2022). Distribution and isotopic signature of 2-alkyl-1,3,4-trimethylbenzenes in the Lower Paleozoic source rocks and oils of Tarim Basin: implications for the oil-source correlation. *Petrol. Sci.* 19, 2572–2582. doi:10.1016/j.petsci.2022.07.014

He, T., Lu, S., Li, W., Tan, Z., and Zhang, X. (2018). Effect of salinity on source rock formation and its control on the oil content in shales in the hetaoyuan formation from the biyang depression, nanxiang basin, Central China. *Energy fuels.* 32, 6698–6707. doi:10.1021/acs.energyfuels.8b01075

He, T. H., Li, W. H., Lu, S. F., Yang, E. Q., Jing, T. T., Ying, J. F., et al. (2023). Quantitatively unmixing method for complex mixed oil based on its fractions carbon isotopes: a case from the Tarim Basin, NW China. *Petrol. Sci.* 20, 102–113. doi:10.1016/j.petsci.2022.07.010

Hu, T., Jiang, F., Pang, X., Liu, Y., Wu, G., Zhou, K., et al. (2024). Identification and evaluation of shale oil micro-migration and its petroleum geological significance. *Petroleum Explor. Dev.* 51, 127–140. doi:10.1016/S1876-3804(24)60010-8

Hu, T., Pang, X., Jiang, F., Zhang, C., Wu, G., Hu, M., et al. (2022). Dynamic continuous hydrocarbon accumulation (DCHA): existing theories and a new unified accumulation model. *Earth-Science Rev.* 232, 104109. doi:10.1016/j.earscirev.2022.104109

Jiang, L., Zhao, W., Bo, D., Hong, F., Gong, Y., and Hao, J. (2023). Tight sandstone gas accumulation mechanisms and sweet spot prediction, Triassic Xujiahe Formation, Sichuan Basin, China. *Petroleum Sci.* 20 (6), 3301–3310. doi:10.1016/j.petsci.2023.07.008

Jiang, Z., Li, Z., Li, F., Pang, X., Yang, W., Liu, L., et al. (2015). Tight sandstone gas accumulation mechanism and development models. *Petroleum Sci.* 12, 587–605. doi:10.1007/s12182-015-0061-6

Lai, J., Wang, G., Cai, C., Fan, Z., Wang, S., Chen, J., et al. (2018a). Diagenesis and reservoir quality in tight gas sandstones: the fourth member of the upper triassic Xujiahe Formation, central Sichuan Basin, southwest China. *Geol. J.* 53 (2), 629–646. doi:10.1002/gj.2917

Lai, J., Wang, G., Wang, Z., Chen, J., Pang, X., Wang, S., et al. (2018b). A review on pore structure characterization in tight sandstones. *Earth-Science Rev.* 177, 436–457. doi:10.1016/j.earscirev.2017.12.003

Li, H., Tang, H., Qin, Q., Zhou, J., Qin, Z., Fan, C., et al. (2019). Characteristics, formation periods and genetic mechanisms of tectonic fractures in the tight gas sandstones reservoir: a case study of Xujiahe Formation in YB area, Sichuan Basin, China. *J. Petroleum Sci. Eng.* 178, 723–735. doi:10.1016/j.petrol.2019.04.007

Li, J., Wang, Y., Song, Z., Wang, M., and Zhao, J. (2024). Mobility of connate pore water in gas shales: a quantitative evaluation on the Longmaxi shales in the southern Sichuan basin, China. *Mar. Petroleum Geol.* 161, 106674. doi:10.1016/j.marpetgeo.2023.106674

Li, P., Hu, Z., Liu, Z., Xu, S., Liu, Z., Wang, A., et al. (2024). Differential controlling on the deep tight sandstone reservoirs: insight from the second member of lower Triassic Xujiahe Formation in Xinchang area, western Sichuan basin, China. *J. Nat. Gas Geoscience* 9 (6), 387–399. doi:10.1016/j.jnggs.2024.10.003

Li, W., Li, J., Lu, S., Song, Z., Wei, Y., Zhang, P., et al. (2022). Evaluation of gas-in-place content and gas-adsorbed ratio using car-bon isotope fractionation model: a case study from Longmaxi shales in Sichuan Basin, China. *Int. J. Coal Geol.* 249, 103881. doi:10.1016/j.coal.2021.103881

Li, W., Wang, J., Jia, C., Lu, S., Li, J., Zhang, P., et al. (2024). Carbon isotope fractionation during methane transport through tight sedimentary rocks: phenomena, mechanisms, characterization, and implications. *Geosci. Front.* 15 (No.6), 101912. doi:10.1016/j.gsf.2024.101912

Liu, J., Liu, Z., Xiao, K., Huang, Y., and Jin, W. (2020). Characterization of favorable lithofacies in tight sandstone reservoirs and its significance for gas exploration and exploitation: a case study of the 2nd Member of Triassic Xujiahe Formation in the Xinchang area, Sichuan Basin. *Petroleum Explor. Dev.* 47 (6), 1194–1205. doi:10.1016/S1876-3804(20)60129-5

Liu, L., Liu, X., Sang, Q., Li, W., Xiong, J., and Liang, L. (2024). Pore-throat structure and fractal characteristics of tight gas sandstone reservoirs: a case study of the second member of the Upper Triassic Xujiahe Formation in Zhongba area, western Sichuan depression, China. *Geol. J.* 59 (6), 1879–1891. doi:10.1002/gj.4975

Liu, X., Chen, H., Chen, Z., Yang, R., Song, L., Bai, M., et al. (2024). Study on characterization and distribution of four regions of tight sandstone condensate gas reservoirs in the depletion development process. *Fuel* 358, 130267. doi:10.1016/j.fuel.2023.130267

Liu, Y., Hu, W., Cao, J., Wang, X., Tang, Q., Wu, H., et al. (2018). Diagenetic constraints on the heterogeneity of tight sandstone reservoirs: a case study on the Upper Triassic Xujiahe Formation in the Sichuan Basin, southwest China. *Mar. Petroleum Geol.* 92, 650–669. doi:10.1016/j.marpetgeo.2017.11.027

Loucks, R. G., Reed, R. M., Ruppel, S. C., and Hammes, U. (2012). Spectrum of pore types and networks in mudrocks and a descriptive classification for matrix-related mudrock pores. *AAPG Bull.* 96 (6), 1071–1098. doi:10.1306/08171111061

Mount, J. F. (1984). Mixing of siliciclastic and carbonate sediments in shallow shelf environments. *Geology* 12 (7), 432–435. doi:10.1130/0091-7613(1984)12<432:MOSACS>2.0.CO;2

Nelson, P. H. (2009). Pore-throat sizes in sandstones, tight sandstones, and shales. *AAPG Bull.* 93 (3), 329–340. doi:10.1306/10240808059

Shi, B., Chang, X., Yin, W., Li, Y., and Mao, L. (2019). Quantitative evaluation model for tight sandstone reservoirs based on statistical methods-A case study of the Triassic Chang 8 tight sandstones, Zhenjing area, Ordos Basin, China. *J. Petroleum Sci. Eng.* 173, 601–616. doi:10.1016/j.petrol.2018.10.035

Wang, Q., Chen, D., Gao, X., Wang, F., Li, J., Liao, W., et al. (2020). Microscopic pore structures of tight sandstone reservoirs and their diagenetic controls: a case study of the Upper Triassic Xujiahe Formation of the Western Sichuan Depression, China. *Mar. Petroleum Geol.* 113, 104119. doi:10.1016/j.marpetgeo.2019.104119

Yang, P., Zhang, L., Liu, K., Cao, B., Gao, J., Qiu, G., et al. (2021). Diagenetic history and reservoir evolution of tight sandstones in the second member of the Upper Triassic Xujiahe Formation, western Sichuan Basin, China. *J. Petroleum Sci. Eng.* 201, 108451. doi:10.1016/j.petrol.2021.108451

Zhang, J., Liu, G., Cao, Z., Tao, S., Felix, M., Kong, Y., et al. (2019). Characteristics and formation mechanism of multi-source mixed sedimentary rocks in a saline lake, a case study of the Permian Lucaogou Formation in the Jimusaer Sag, northwest China. *Mar. Petroleum Geol.* 102, 704–724. doi:10.1016/j.marpetgeo.2019.01.016

Zhang, Y., Zhang, R., Qu, L., Wu, H., Dai, Q., Zhang, Z., et al. (2024). Development characteristics of natural fractures in tight sandstone reservoirs and their controlling factors: upper Triassic Xujiahe Formation, western Sichuan Basin. *Front. Earth Sci.* 12, 1430091. doi:10.3389/feart.2024.1430091

Zhao, J., Zhang, L., Tian, L., Yang, Y., and Chen, G. (2024). Distributary channel type and high-quality reservoirs in tight sandstone—a case study on the outcrops and reservoirs of Xujiahe formation in Western Sichuan Basin. *Energy Sci. and Eng.* 12 (11), 5119–5144. doi:10.1002/ese3.1940

Zou, C., Zhu, R., Liu, K., Su, L., Bai, B., Zhang, X., et al. (2012). Tight gas sandstone reservoirs in China: characteristics and recognition criteria. *J. Petroleum Sci. Eng.* 88, 82–91. doi:10.1016/j.petrol.2012.02.001